

ON THE INTERPRETATION OF THE BROAD-BAND MILLIMETER-WAVE FLUX FROM ORION

E. C. SUTTON,¹ GEOFFREY A. BLAKE,² C. R. MASSON,¹ AND T. G. PHILLIPS¹

Received 1984 April 3; accepted 1984 May 31

ABSTRACT

Spectral observations of the core of Orion A at wavelengths around 1.3 mm show a high density of strong, broad emission lines. The combined flux in lines with peak antenna temperatures stronger than 0.2 K accounts for approximately 40% of the broad-band millimeter-wave flux from the region. Thus the broad-band flux from Orion A is in large part due to sources other than dust emission.

Subject headings: interstellar: matter — nebulae: Orion Nebula

I. INTRODUCTION

The broad-band submillimeter flux from Orion A has been studied by Keene, Hildebrand, and Whitcomb (1982) and by Elias *et al.* (1978). Taken together, their data imply a flux density of about 128 Jy at 1 mm in a 0.6 beam with a spectral index of about 3. This has generally been interpreted as optically thin emission from dust grains, the steep spectral index being in part due to the steep dust opacity law.

It has been known also that Orion has emission from a large number of strong molecular lines. Recently, Sutton *et al.* (1984) have systematically surveyed the line emission between 215 and 247 GHz. The data show several hundred strong, broad emission lines which in several places blend together to obscure any underlying continuum. The combined emission from these lines is equivalent to that of a continuum with antenna temperature of 0.25 K for a 0.6 beam, which is generally comparable to the total broad-band flux from the region. Thus it is important to examine carefully the calibrations of these data in order to determine whether the bulk of the submillimeter flux should be attributed to line emission instead of dust emission.

II. RESULTS AND CALIBRATION

a) Emission-Line Flux Density

The data of Sutton *et al.* (1984) show over 500 resolvable lines in the frequency interval 215–247 GHz ranging in temperature from about 100 K (the $J = 2-1$ line of ^{12}CO) down to the noise level of about 0.2 K. A compressed view of the spectrum is presented in Figure 1. Line widths present vary from $\sim 4 \text{ km s}^{-1}$ (3 MHz) for the “spike” components of the gas out to $\sim 100 \text{ km s}^{-1}$ (77 MHz) for the broad “plateau” emission. Approximately half of the lines have an intermediate $\sim 12 \text{ km s}^{-1}$ (9 MHz) line width and are attributed to material in the Orion “hot core.” Averaged over the frequency range searched, these lines contribute approximately 0.25 K to the broad-band emission. The $J = 2-1$ line of ^{12}CO alone contributes $\sim 0.05 \text{ K}$ of this emission.

¹Department of Physics, California Institute of Technology.

²Department of Chemistry, California Institute of Technology.

The spectral measurements were calibrated using a standard chopper wheel technique, with beam efficiencies determined by observing the Moon and planets. Sutton *et al.* (1984) reduced their data to a scale of corrected antenna temperature using an efficiency of 0.85, appropriate for emission from spatially extended sources (sources several times larger than the 0.5 beam). Since the “hot core” and “plateau” lines arise from more compact regions, a lower efficiency factor should be used to derive proper main beam brightness temperatures for these components. In general, because of the different sized emitting regions it will not be possible to apply a single flux density or temperature scale which is appropriate for all the lines.

For the present discussion, line fluxes have been calibrated directly from measurements of Saturn. Saturn is small compared to the main beam, a fact which is also known to be true for the plateau component in Orion (Plambeck *et al.* 1982; Friberg 1984; Masson *et al.* 1984). Plateau emission dominates the line fluxes seen here. As a typical example of the calibration, in 1983 May Saturn subtended a diameter of 0.30. Assuming a physical temperature of 160 K, this implies a flux density at 1.3 mm of 1500 Jy. The measured antenna temperature of Saturn under these conditions was 13.3 K (no correction for efficiency). Measurements of Venus and Jupiter (the latter is partially resolved by the main beam) provide consistent calibration within $\pm 20\%$. With this calibration the average flux due to lines stronger than 0.2 K is 25 Jy at a flux-weighted mean wavelength of 1.3 mm. The limited 260 GHz data of Blake *et al.* (1984) clearly show much stronger line emission, as would be generally expected for lines arising in regions of high excitation. With a similar calibration, the average line flux density at 1.15 mm is 51 Jy. These results are plotted in Figure 2.

b) Broad-Band Flux Density

The total broad-band flux (lines plus continuum) from Orion can be determined from the same set of measurements. For comparison with the line fluxes, this is the best procedure since the observations were made with the same beam size, wavelength, and pointing errors as the spectral line data.

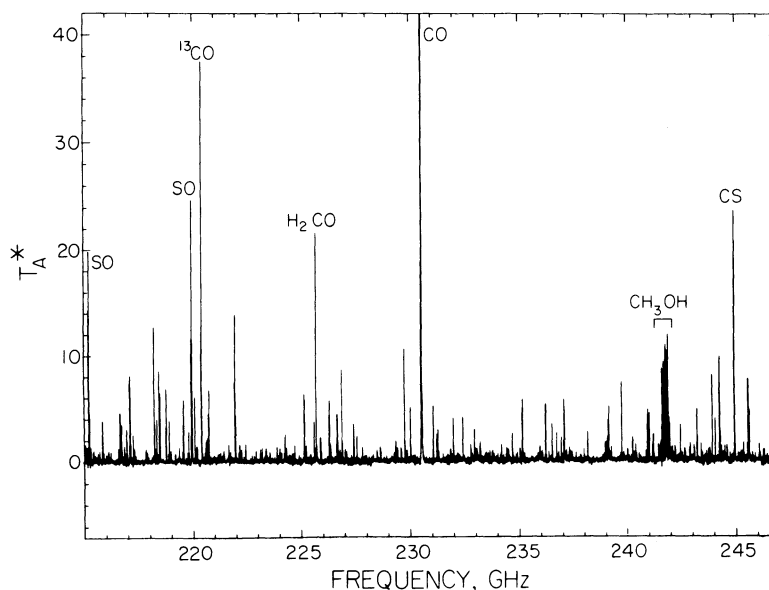


FIG. 1.—Spectrum of Orion A from 215 to 247 GHz. Data were obtained with a typical receiver noise temperature of 500 K (SSB) and backend coverage of 527 MHz. The original spectral resolution was 1.03 MHz (1.3 km s^{-1}). Spectral resolution in this plot is degraded by about a factor of 10.

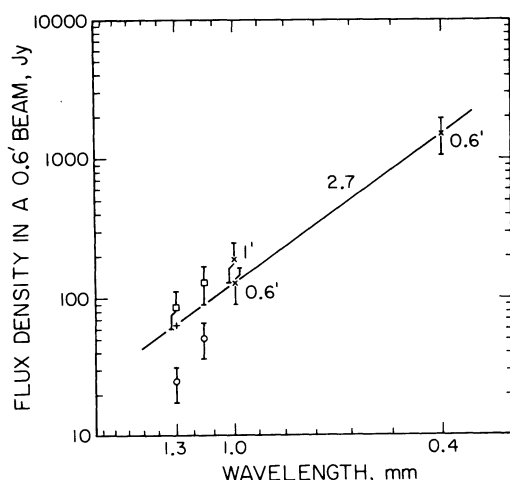


FIG. 2.—Broad-band and spectral line flux densities in a 0.6' beam centered on BN. Open circles show the line fluxes measured by Sutton *et al.* (1984) and Blake *et al.* (1984). Open boxes indicate the total broad-band fluxes measured simultaneously. Crosses represent the broad-band fluxes of Keene, Hildebrand, and Whitcomb (1982) and Elias *et al.* (1978), the latter both for a 1' beam and corrected for a 0.6' beam. Plus sign represents the extrapolation of these short wavelength measurements to 1.3 mm.

However, some additional uncertainties were introduced since the spectral line system was not well optimized for continuum observations. The measured broad-band flux was 86 Jy at 1.3 mm with an uncertainty of about $\pm 15\%$ on top of an overall calibration error of $\pm 20\%$.

This value for the broad-band flux can be compared with the various values in the published literature. The $400 \mu\text{m}$ emission from the core of Orion A has been measured and mapped with 0.6' resolution by Keene, Hildebrand, and Whitcomb (1982). They show that the submillimeter emission consists of an extended component plus two major compact

sources. The flux density at BN is 1500 Jy within a 0.6' beam, with an overall calibration uncertainty of $\pm 30\%$. Previously, the 1 mm emission from Orion was measured by Westbrook *et al.* (1976) and recalibrated by Elias *et al.* (1978). They derived a flux density of 188 Jy in a 1' beam. Assuming that the 1 mm emission has the same spatial distribution as the $400 \mu\text{m}$ emission, it is possible to estimate the 1 mm flux density in a 0.6' beam by using the mapping data of Keene, Hildebrand, and Whitcomb (1982). The result is an estimated flux density of 128 Jy for the smaller beam. Combined with the $400 \mu\text{m}$ result, this implies a spectral index of 2.7 between 0.4 mm and 1 mm. This is similar to but smaller than the spectral index estimated by Elias *et al.* (1978). Extrapolating with this spectral index to 1.3 mm, the wavelength of the spectral line observations, gives a flux density of 63 Jy in a 0.6' beam. The various broad-band fluxes are plotted in Figure 2. Comparison with the line flux indicates that 30%–40% of the total flux may be accounted for as line emission. This, however, is a lower limit since the line flux is based only on those lines stronger than 0.2 K.

III. DISCUSSION

a) Extrapolation to Weaker Lines

The calculations above have considered only those lines strong enough to be individually detected, i.e., those with peak antenna temperatures stronger than about 0.2 K. There will be a large number of weaker lines present which cannot be seen because of the noise level in the spectrum and because of the overlapping of stronger lines. Even at the 0.2 K level there are large regions of the spectrum in which the baseline cannot be clearly seen due to the overlapping wings of strong lines.

Some weaker lines can be predicted with some precision because they involve transitions with weaker matrix elements or are between more highly excited states of well-known species. But the general problem of predicting the number of

weaker lines cannot be solved precisely, since there will be contributions from new molecular species with completely unknown abundances. A naive approach is to examine the distribution of line intensities and to extrapolate to weaker values. This distribution has been calculated for the 215–247 GHz data and is presented in Figure 3. The number of lines falls off steadily with increasing antenna temperature with a more rapid falloff above about 10 K as expected due to saturation effects. At the low-temperature end there seems to be a serious undercounting of lines in the 0.25–0.5 K interval. The slope at the low-temperature end is around -0.8 , indicating a converging contribution from the weaker lines. The indicated extrapolation predicts that the line flux has been underestimated by about 30% by not including the weaker lines. This raises the line contribution to $\sim 45\%$ of the total flux.

This treatment is somewhat uncertain since it does not take into account the variety of line widths present. The individual statistics for plateau, hot core, and spike components are unfortunately insufficient to determine their distributions separately. However, it is likely that the missing lines in the low-temperature bins are mostly broad plateau lines, since weak broad lines are the easiest to miss in a crowded spectrum with a slowly varying baseline. If it is assumed that the missing lines are from the plateau source, then the line flux should be increased by a factor of about 1.7, and it would then account for 60% of the total flux.

b) Spectral Index

The spectral index determined from the broad-band flux data is about 2.7. A similar index also applies to the spectral line data, although the value is somewhat less certain due to the limited wavelength range and the possible biases introduced by a few strong lines and bands (e.g., the $J = 2-1$ line of CO and the $J = 5-4$ band of CH_3OH).

The observed spectral index can be readily explained either by dust emission or line emission. For example, the slope is nearly that expected for optically thin emission from warm dust grains ($T_d \geq 20$ K) with a dust emissivity law of λ^{-1} . The line emission estimate is more difficult due to the complex ensemble of molecules present. For each type of molecule the variation in line flux with frequency will depend on the symmetry of the molecule and its column density (and hence optical depth). A linear molecule will have a series of evenly spaced lines, corresponding to the different values of J , the total angular momentum, whose optical depths vary as ν^2 . For a fixed velocity dispersion the line widths also vary as ν . Thus the spectral flux variation for such a molecule could range from ν^3 (optically thick) to ν^5 (optically thin) for the case of thermal excitation to a temperature $T_{\text{ex}} \geq 20$ K. Lack of adequate excitation will tend to flatten the spectrum at sufficiently high frequencies. Symmetric and asymmetric top molecules will show a more rapid flux variation, since for large values of J the line strength of an entire $J \rightarrow J-1$ band will vary approximately as J^2 instead of as J for a linear molecule. Thus the spectral index data can be readily explained by a mixture of various molecular species with various optical depths. Since the line flux is dominated by asymmetric top molecules such as SO_2 , the relatively low index of 2.7 suggests most of the emission is in optically thick lines.

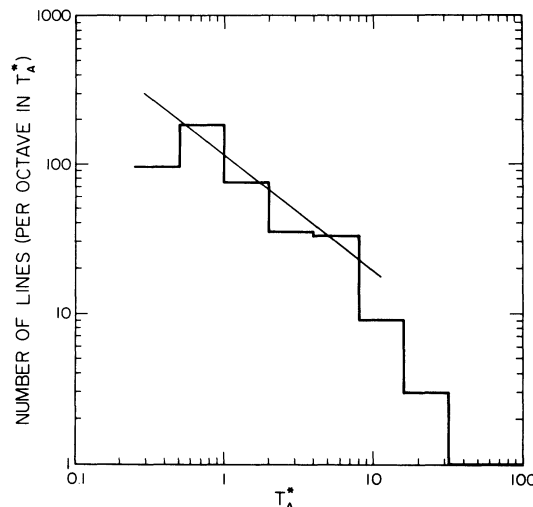


FIG. 3.—Distribution of peak corrected antenna temperatures for lines in the 215–247 GHz band.

c) Source Size

An estimate of the size of the Orion plateau source may be obtained for the SO_2 lines from the conclusion that the strongest of these are optically thick. The strongest SO_2 lines have peak antenna temperatures of ~ 20 K. Since the excitation temperature for SO_2 is thought to be about 90 K (Schloerb *et al.* 1983) this implies a source size of approximately $14''$ diameter. This is in good agreement with previous measurements of the plateau size (Plambeck *et al.* 1982; Masson *et al.* 1984).

d) Similarities between Line Maps and Broad-Band Maps

Since line emission accounts for much of the broad-band flux from Orion, then maps of emission in the dominant molecular species should look similar to the broad-band “continuum” maps. The line emission from 215–247 GHz is dominated by SO_2 ($\sim 30\%$ of the flux) and CO ($\sim 25\%$ of the flux). SO_2 emission is known to come from the plateau source which is spatially compact and located in the vicinity of IRC2. The CO emission has a large plateau component as well but also displays significant spatially extended emission. Other major molecular species (e.g., SO and CH_3OH) follow one or the other of these spatial distributions.

The $400 \mu\text{m}$ map of Keene, Hildebrand, and Whitcomb (1982) displays this general pattern of spatially compact emission centered near IRC2 and additional extended emission. The chief difference is the presence in the $400 \mu\text{m}$ map of a second compact source well to the south ($-5^\circ 25' 50''$). This southern source is prominent in some molecular line maps, particularly a ^{13}CO map of Schloerb and Loren (1982) and most strongly in an HCO^+ ($J = 3-2$) map of Wootten and Loren (1984).

e) Other Molecular Clouds

Similar results may hold for other molecular clouds. However, in cooler clouds with narrower line widths, the molecular

emission would be restricted to the optically thick line cores. Thus, for similar amounts of molecular material the line flux would be somewhat reduced relative to any true continuum flux.

III. CONCLUSIONS

A high spectral density of emission lines is observed in Orion A at wavelengths around 1.3 mm. These lines are sufficiently strong and broad that in many places they obscure the underlying continuum. The combined flux in the strongest of these lines is estimated to be approximately 40% of the

broad-band flux. Accounting for weaker, presently undetected lines increases this to about 60%. Within the errors, line emission could be the dominant contribution to the millimeter-wave flux.

Single-dish millimeter-wave astronomy at the Owens Valley Radio Observatory is supported by NSF grant AST-8214693. The authors would like to thank R. E. Miller of AT & T Bell Laboratories, Murray Hill, for supplying the junctions used in this work. The authors are also grateful to D. P. Woody and S. L. Scott for their assistance and to Jocelyn Keene for helpful discussions.

REFERENCES

- Blake, G. A., *et al.* 1984, in preparation.
 Elias, J. H., *et al.* 1978, *Ap. J.*, **220**, 25.
 Friberg, P. 1984, *Astr. Ap.*, **132**, 265.
 Keene, J., Hildebrand, R. H., and Whitcomb, S. E. 1982, *Ap. J. (Letters)*, **252**, L11.
 Masson, C. R., *et al.* 1984, *Ap. J. (Letters)*, **283**, L37.
 Plambeck, R. L., Wright, M. C. H., Welch, W. J., Bieging, J. H., Baud, B., Ho, P. T. P., and Vogel, S. N. 1982, *Ap. J.*, **259**, 617.
 Schloerb, F. P., Friberg, P., Hjalmarson, A., Höglund, B., and Irvine, W. M. 1983, *Ap. J.*, **264**, 161.
 Schloerb, F. P., and Loren, R. B. 1982, *Symposium on the Orion Nebula to Honor Henry Draper*, ed. A. E. Glassgold, P. J. Huggins, and E. L. Schucking, *Ann. NY Acad. Sci.*, **395**, 32.
 Sutton, E. C., *et al.* 1984, in preparation.
 Westbrook, W. E., Werner, M. W., Elias, J. H., Gezari, D. Y., Hauser, M. G., Lo, K. Y., and Neugebauer, G. 1976, *Ap. J.*, **209**, 94.
 Wootten, A., and Loren, R. B. 1984, in preparation.

GEOFFREY A. BLAKE and T. G. PHILLIPS: Downs Laboratory of Physics 320-47, California Institute of Technology, Pasadena, CA 91125

C. R. MASSON: Downs Laboratory of Physics 405-47, California Institute of Technology, Pasadena, CA 91125

E. C. SUTTON: Space Sciences Laboratory, University of California, Berkeley, CA 94720